machines

MDPI

Article

Experimental Validation of a Driver Monitoring System

María Garrosa [1,*], Marco Ceccarelli [2], Vicente Díaz [1] and Matteo Russo [2]

[1] Mechanical Engineering Department, Universidad Carlos III de Madrid, Avda. de la Universidad 30, 28911 Leganés, Spain; vdiaz@ing.uc3m.es
[2] Department of Industrial Engineering, Università di Roma Tor Vergata, Via del Politecnico 1, 00133 Rome, Italy; marco.ceccarelli@uniroma2.it (M.C.); matteo.russo@uniroma2.it (M.R.)
* Correspondence: mgarrosa@ing.uc3m.es; Tel.: +34-91-624-6248

Abstract: This paper presents an analysis of the risk of neck injury in vehicle occupants as a consequence of an impact. A review of the formulation of indexes that are used in the assessment and investigation of neck injury risk is discussed with the aim of providing a new, more appropriate index using suitable sensorized equipment. An experimental analysis is proposed with a new driver monitoring device using low-cost sensors. The system consists of wearable units for the head, neck, and torso where inertial measurement sensors (IMU) are installed to record data concerning the occupant's head, neck, and torso accelerations while the vehicle moves. Two laser infrared distance sensors are also installed on the vehicle's steering wheel to record the position data of the head and neck, as well as an additional IMU for vehicle acceleration values. To validate both the device and the new index, experiments are designed in which different sensorized volunteers reproduce an emergency braking maneuver with an instrumented vehicle at speeds of 10, 20, and 30 km/h before the beginning of any braking action. The neck is particularly sensitive to sudden changes in acceleration, so a sudden braking maneuver is enough to constitute a potential risk of cervical spine injury. During the experiments, large accelerations and displacements were recorded as the test speed increased. The largest accelerations were obtained in the experimental test at a speed of 30 km/h with values of 19.17, 9.57, 9.28, and 5.09 m/s^2 in the head, torso, neck, and vehicle, respectively. In the same experiment, the largest displacement of the head was 0.33 m and that of the neck was 0.27 m. Experimental results have verified that the designed device can be effectively used to characterize the biomechanical response of the neck in car impacts. The new index is also able to quantify a neck injury risk by taking into account the dynamics of a vehicle and the kinematics of the occupant's head, neck, and torso. The numerical value of the new index is inversely proportional to the acceleration experienced by the vehicle occupant, so that small values indicate risky conditions.

Keywords: biomechanics; injury criteria; testing design; experimental validation; risk evaluation

Citation: Garrosa, M.; Ceccarelli, M.; Díaz, V.; Russo, M. Experimental Validation of a Driver Monitoring System. *Machines* **2023**, *11*, 1060. https://doi.org/10.3390/machines11121060

Academic Editor: Jiangjian Xiao

Received: 12 October 2023
Revised: 20 November 2023
Accepted: 27 November 2023
Published: 29 November 2023

1. Introduction

Nowadays, nonfatal injuries are a worldwide public health problem. Impact injury investigation and the analysis of experimentally based biomechanics play key roles in the mitigation of injuries caused by road traffic crashes. In general, in low-speed rear-end crashes, the head of the impacted vehicle occupant moves relative to the torso, causing distortion of the neck, meaning the cervical spine is the most vulnerable area and can face minor (sprains/strains), moderate (intervertebral disc derangement), and severe (fractures, dislocations, and spinal cord injuries) injuries [1]. The frequency of these injuries is inversely proportional to their severity, meaning the most common and least severe injuries are musculoligamentous strains which are known as whiplash. Less common injuries are disc injuries and vertebral fractures, and the least common are spinal cord injuries. Whiplash injuries include skin, blood vessel, muscle, ligament, nerve, and intervertebral disc injuries [2] and can cause headache, neck pain or stiffness, arm pain and paresthesia,

temporomandibular dysfunction, visual disturbances, memory and concentration problems, and psychological distress [3]. In addition, whiplash causes enormous economic costs to society [4]. The analysis of the mechanisms of whiplash is complicated by the complex structure of the cervical spine and the various impact conditions. Numerous investigation reports can be found in the literature that have attempted to characterize the cervical spine biomechanical response. Many of these investigations have tested animals [5], human volunteers [6], human cadavers [7], crash-test dummies [8], articulated artificial necks [9], and computational models [10–12].

To analyze the risk and severity of cervical injuries in vehicle impacts there are different injury criteria such as the neck injury criterion (NIC) [5], neck protection criterion (N_{km}) [13], neck injury criteria (N_{ij}) [14], lower neck load index (LNL) [15], intervertebral neck injury criterion (IV-NIC) [16], neck displacement criterion (NDC) [17], whiplash injury criterion (WIC) [18], and head-to-torso rotation [19].

This paper is an extended revised version of the paper presented at the MESROB 2023 conference [20], with more results and discussions addressing an experimental evaluation of the injury risk in a car accident.

In this paper, a new criterion is proposed through a detailed analysis of the different aspects to be considered in the analysis of the risk of injury to the head–neck–torso system as a consequence of a vehicle impact. A low-cost device to monitor the driver of a vehicle and experimental tests consisting of a series of emergency braking maneuvers at low speed without experiencing an impact are designed to validate the new criterion. No impact does not mean that there is no risk of injury to occupants, as pointed out in [21]. Sudden braking is sufficient to cause cervical spine injury because the neck is very sensitive to sudden changes in acceleration [22]. In emergency braking, the head and torso move with a delay between them due to their different inertia. This implies that some vertebrae are in flexion while others are in hyperextension, with the possibility of producing a cervical injury.

Experimental tests, carried out with the participation of volunteers, consisted of emergency braking at speeds of 10, 20, and 30 km/h on a flat track following a straight trajectory. In all tests, the occupant sits in the normal driving position, looking straight ahead and using a three-point seatbelt to connect her or his movement with that of the vehicle. The seatbelt is very effective when the vehicle is moving at high speeds; however, it can increase the risk of whiplash injury at low speeds, as indicated in [23].

With the main goal of characterizing the biomechanical response of the neck in terms of acceleration and displacement, the acceleration of the vehicle occupant's head, neck, and torso, as well as the acceleration of the vehicle, are recorded during the experiments using IMUs. Head and neck displacement data are also recorded using laser infrared distance sensors placed inside the vehicle. The paper focuses on the successful usage of these low-cost sensors to monitor a driver and to obtain information on the chosen parameters to formulate a new index. The results obtained with the new index demonstrate its effectiveness in providing a numerical estimations of the whiplash risk.

The manuscript is organized as follows. Section 1.1 introduces the biomechanics of the whiplash motion. Section 1.2 reviews the indexes for neck injury risk assessment. Section 2 outlines the requirements and design issues for a monitoring system. It also presents the methodology, including a description of the experimental test setup, the definitions of the experiments, and the data collection and analysis. The results are discussed in Section 3. Finally, the conclusion drawn from the results is presented in Section 4.

1.1. Biomechanics of a Whiplash Motion

The classical whiplash injury hypothesis is the result of a hyperextension movement of the neck [24–26]. The analysis of the neck motion of a vehicle occupant during a rear-end or frontal collision, both of which may result in soft-tissue injuries to the neck, shows complex kinematics. The resulting motion of an occupant during a rear-end collision can be divided into three different phases, as shown in Figure 1. During the first phase, known as retraction, an occupant is pushed forward by the seat back. The transmission of forces

and contact takes place at the shoulders. Moving due to inertia, the head retracts, i.e., it moves backwards without rotation about the lateral axis, and is placed behind the torso. Thus, the lower cervical spine is forced into extension and the upper cervical spine is forced into flexion. This deformation of the neck is known as an S-shaped configuration and is considered crucial to the mechanism of injury [27–31]. Following the S-shaped configuration, the head starts rotating backwards, which, in turn, leads to the extension of the entire cervical spine. The retraction phase finishes with the maximum extension of the cervical spine. The next phase is a forward movement, which is characterized by a change in the direction of movement, i.e., the head, neck, and torso move forward. When the occupant returns to a position that, in the sagittal direction, is equal to the initial position before the impact, the forward motion phase is completed and the seatbelt restraint phase begins. An occupant is restrained by the safety belt in such a way that the thoracic spine is stopped while the head moves forward. This produces an inverted S-shaped configuration of the neck. However, the effect is less pronounced than the S-shaped configuration experienced in the first phase. This is due to damping of restraining forces by the rib cage and to the fact that more vertebrae are involved in this second S-shaped configuration, which gives lower loads on the individual vertebrae. Finally, the kinematic phases conclude with a global flexion of the cervical spine.

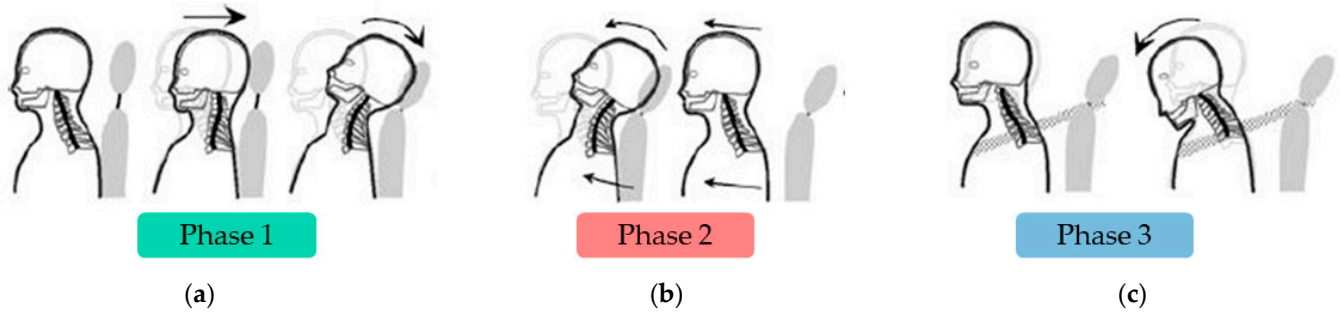

Figure 1. Kinematic phases in a rear impact: (**a**) Retraction; (**b**) Forward movement; (**c**) Belt restraint.

Similar kinematic phases apply for frontal collisions, including the inverted S-shape configuration.

1.2. Injury Criteria

Among the numerous injury criteria available for assessing the risk of injury during an impact, the following presents a summary of the main formulations.

The neck injury criterion (NIC) is widely utilized for detecting soft tissue injuries in the neck resulting from rear-end collisions [5]. This criterion predicts the relationship between spinal cord nerve tissue damage and pressure gradients. Based on the assumption that pressure gradients caused by a sudden change in the fluid flow inside the fluid compartments of the cervical spine are related to neck injuries, $NIC(t)$ was defined as follows [5].

$$NIC(t) = 0.2 \cdot a_{rel}(t) + v_{rel}(t)^2 \quad (1)$$

Here, a_{rel} and v_{rel} are the relative horizontal acceleration and velocity between the bottom (T1) and top (C1) of the cervical spine. The constant, 0.2 m, represents an approximation of the length of the neck. The threshold value above which a significant risk of a minor neck injury is considered to exist was set at 15 m^2/s^2 [5]. This criterion becomes less stringent when the head is no longer parallel to T1, at head extension angles of approximately 20–30°.

The neck protection criterion ($N_{km}(t)$) was developed to detect neck soft tissue injuries in rear-end impacts [13]. It is based on the assumption that a linear combination of loads and moments describes best the neck loading according to the expression [13]:

$$N_{km}(t) = \frac{F_x(t)}{F_{int}} + \frac{M_y(t)}{M_{int}} \tag{2}$$

where $F_x(t)$ and $M_y(t)$ are the shear force and the flexion/extension bending moment, respectively, as measured with a load cell at the upper neck. F_{int} and M_{int} represent the critical intercept values for normalization.

The neck injury criteria (N_{ij}) was developed by the US National Highway Traffic Safety Administration (NHTSA) to assess severe cervical injuries caused by frontal impacts, and is shown in the form [14]:

$$N_{ij} = \frac{F_Z}{F_{int}} + \frac{M_Y}{M_{int}} \tag{3}$$

where F_Z and M_Y are the axial force and the flexion/extension sagittal bending moment, respectively. F_{int} and M_{int} are the critical intercept values of force and moment that are used for normalization.

The lower neck load index ($LNL(t)$) considers three force and two moment components that are measured at the base of the neck. Therefore, the evaluation requires a dummy equipped with a load cell at the lower part of the neck to compute the expression [15]:

$$LNL(t) = \left| \frac{\sqrt{\left(M_{y_{lower}}(t)\right)^2 + \left(M_{x_{lower}}(t)\right)^2}}{C_{moment}} \right| + \left| \frac{\sqrt{\left(F_{y_{lower}}(t)\right)^2 + \left(F_{x_{lower}}(t)\right)^2}}{C_{shear}} \right| + \left| \frac{F_{z_{lower}}(t)}{C_{tension}} \right| \tag{4}$$

where $F_i(t)$ and $M_i(t)$ are the force and moment components, respectively. The denominators represent intercept values for a rear-impact dummy (RID).

The whiplash injury criterion (WIC) only takes into account injury mechanisms that are associated with S-shaped neck configurations and is expressed as [18]:

$$WIC = M_{yOC} - M_{ylw} \tag{5}$$

where M_{yOC} represents the y moment around the occipital condyle and M_{ylw} represents the y moment measured at the T1 load cell.

A common limitation of injury criteria is the fact that they can only be established under controlled conditions, i.e., in experiments. Real collisions cannot be assessed retrospectively by these criteria, because neck loads cannot be measured.

It can be noted that these criteria do not directly take into account neck movement. Neither do they consider vehicle-specific factors, such as vehicle acceleration, nor the specific biomechanics of an occupant. These factors can be relevant when assessing whiplash injuries.

2. Materials and Methods

2.1. Issues and Requirements

Several issues arise in the analysis of car impacts and their consequences for occupants. First of all, experiments with human volunteers involving a situation with loads that can cause injury are not permitted. Therefore, experiments with volunteers are restricted only to the low severity range, i.e., well below any level considered to be possibly injurious. Ethical considerations also limit how and what type of experiments can be performed with volunteers. Difficulties with instrumentation arise as well because the sensors often cannot be installed in the desired location, e.g., at the head or neck center of gravity, and it can be difficult to fix them properly on the volunteer. Finally, other problems include the large number of possible injury mechanisms and injuries that can occur.

The design of a vehicle driver monitoring system has to address certain requirements. The device has to be able to integrate several sensors to monitor both the displacement of the head and neck and the acceleration of the occupant's head, neck, and torso. The information from the sensors has to be able to be acquired with an appropriate sampling

rate and processed in real time. It has to consist of low-cost devices to minimize the cost of implementation in commercial vehicles. The system should provide a non-intrusive signal measurement system that allows a driver to practice her/his normal movements without any restriction. Finally, an architecture has to be designed that integrates all of the above requirements, guaranteeing high reliability.

The issues and requirements for experimental characterization of the human biomechanical response during a vehicle impact can be summarized as in Figure 2.

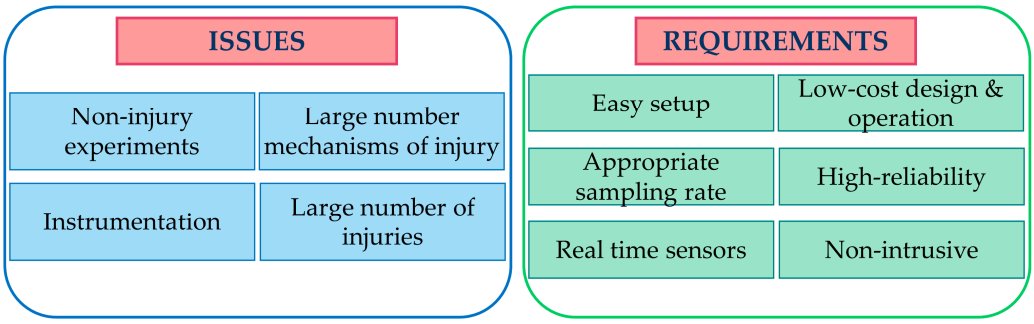

Figure 2. Diagram of the issues and requirements for analyzing vehicle impact injuries.

2.2. Monitoring Design

Choosing appropriate sensors when instrumenting a vehicle and occupants is important for an experimental evaluation of the proposed index in Equation (6).

Such a device includes a series of sensors in order to characterize the risk of neck injury in a low-cost, efficient, and user-oriented structure, based on previous experiences in [32–34]. The monitoring system consists of a head strap, a neck strap, and a torso waistcoat, as shown in Figure 3. The units are sensorized using low-cost, market-available components. Four MPU-6050 IMUs [35] and two VL53L0X infrared laser sensors [35] are installed. In addition, the I2C multiplexer TCA9548A [35] is used to expand the I2C bus ports to connect I2C sensors [35] with the same address to a microcontroller.

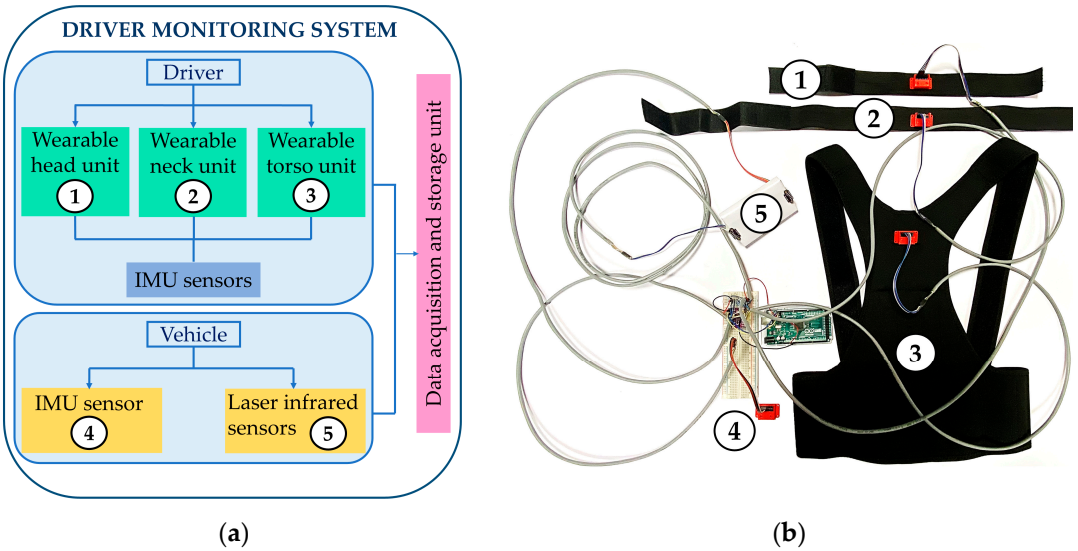

(**a**) (**b**)

Figure 3. Design of the proposed monitoring device: (**a**) Scheme; (**b**) Lab setup.

The technical specifications of the sensors used are listed in Table 1. The monitoring system is provided with connections to a laptop that stores and processes the acquired data by means of an appropriate code.

Table 1. Technical specifications of the monitoring device sensors.

Technical Specification	IMU MPU-6050 [35]	Laser Infrared VL53L0X [35]	Multiplexer TCA9548A [35]
Operating voltage	2.375–3.46 V	2.6–3.5 V	1.65–5.5 V
Range	±16 g	50–1200 mm	0–400 kHz
Main specifications	Sensitivity: 2048 LSB/g	Field of view (FOV): 25° 940 nm laser vertical cavity surface-emitting laser (VCSEL)	1–8 Bidirectional translating switches
Size	16.5 × 20 mm	10.5 × 13.3 mm	30.6 × 17.6 mm
Cost	1.79 €	4.79 €	4.99 €

The signals obtained by the sensors during experiments are collected by the Arduino MEGA 2560 microcontroller [36]. The sensors communicate with the microcontroller via the I2C bus. The measurements of the sensors are transferred to the microcontroller and then transmitted to the connected laptop. The specifications of the Arduino MEGA 2560 board are listed in Table 2. Figure 4 shows the electronic design with the connections of the sensors to the equipment used to perform the data acquisition during the experimental tests. The used sampling frequency for data acquisition is 33 Hz.

Table 2. Technical specifications of the Arduino MEGA 2560 board.

Technical Specification	Arduino MEGA 2560 [36]
Microcontroller	ATmega 2560
Operating voltage	5 V
Analog input pins	16
Digital input/output pins	54
Flash memory	256 kB
Static random access memory (SRAM)	8 kB
Processor speed	16 MHz
Size	101.52 × 53.3 mm
Cost	46.12 €

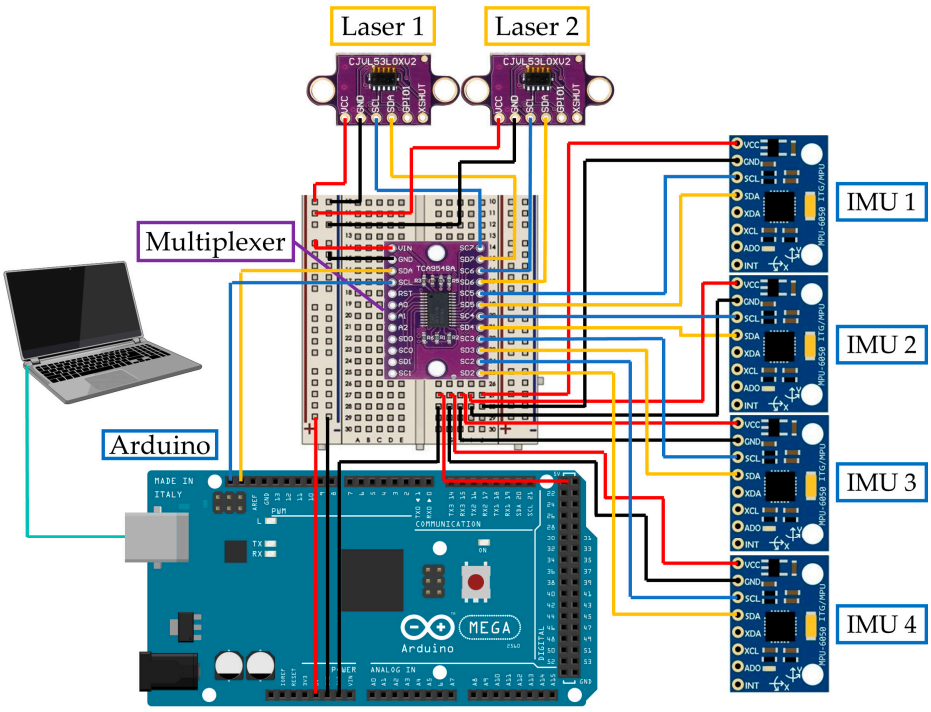

Figure 4. Electronic design of the driver monitoring system in Figure 3, Table 1.

2.3. New Injury Criterion

A new criterion called $NHIC_2$ (neck–head injury criterion 2) is formulated considering the parameters evaluated in the previous experiences. This criterion considers neck displacement as an improvement of the expression in [37,38]. It is calculated as:

$$NHIC_2 = \frac{(m_v + m)\cdot a_v}{m\cdot(V_v)^2}\cdot\frac{a_{hmax}}{a_{nmax}}\cdot\left(\left(X_{hf} - X_{hi}\right) + \left(X_{nf} - X_{ni}\right)\right)\cdot 1000 \quad (6)$$

where m_v is the vehicle weight, m is the occupant weight, a_v is the maximum vehicle acceleration, V_v is the vehicle speed at the moment of the experiment, a_{hmax} is the maximum head acceleration, a_{nmax} is the maximum neck acceleration, X_{hf} is the position of the head after the test, X_{hi} is the initial position of the head, X_{nf} is the position of the neck after the test, and X_{ni} is the initial position of the neck.

The new criterion in Equation (6) is conceived for a procedure that is designed to improve injury risk analysis and to assess the impact effects in more detail by using more parameters than in existing approaches thanks to improved sensorization.

2.4. Design of Experimental Tests

This section describes the new methodology proposed for the design of the experimental phase using the instrumentation shown in Figures 3 and 4.

The experiments were planned with volunteers without neck or head injuries. The experiments were designed to avoid possible damage and injury to the volunteer. A condition of participation in the experiment was that the volunteer was in good health and had no neck or head injuries that could be aggravated by participation in the experiment. The experimental tests were divided into the different phases as shown in Figure 5 with several steps, as follows.

Step 1. Experiment explanation. Before the experiment, participants were informed about the nature, purpose, methods, and risk of the study and then asked to complete a questionnaire on anthropometric information such as their gender, age, height, and weight, among other factors. The subjects signed a consent form that contained a detailed description of the experiment, its duration, and the objectives of the research. However, participants were always given the opportunity to leave the experiment at any time during the experiment if they wanted.

Step 2. Vehicle instrumentation. The IMU sensor MPU-6050 was fixed at the center of gravity of the vehicle, in a horizontal position (level with the ground) and oriented with the main direction of movement, to monitor the acceleration of the car. In addition, the two high-precision VL53L0X laser infrared sensors were placed on the top of the steering wheel to determine the trajectory and relative motion of the head and neck. The laser infrared sensors were positioned properly on the steering wheel for the experiments, taking into account the 25° conical measuring range of the sensor to ensure the detection of neck and head displacement. An action camera with slow motion recording was also installed to provide a visual record of the occupant's movement during the experiment. Figure 6 shows the sensors installed in the vehicle.

Step 3. Volunteer sensorization. The occupant was outfitted with the wearable units for the head, neck, and torso to obtain the acceleration measurements of the head-front, neck, and torso. Figure 7 shows an occupant sensorized with the wearable units. The axes used for head movement are mediolateral (Y-axis), anterior–posterior (X-axis), and vertical (Z-axis). Thus, the flexion–extension movement corresponds to the rotation in the sagittal plane around the Z-axis. Before starting the measurements, preliminary familiarization tests were performed to explain the experiment and to get the participant used to the instrumentation.

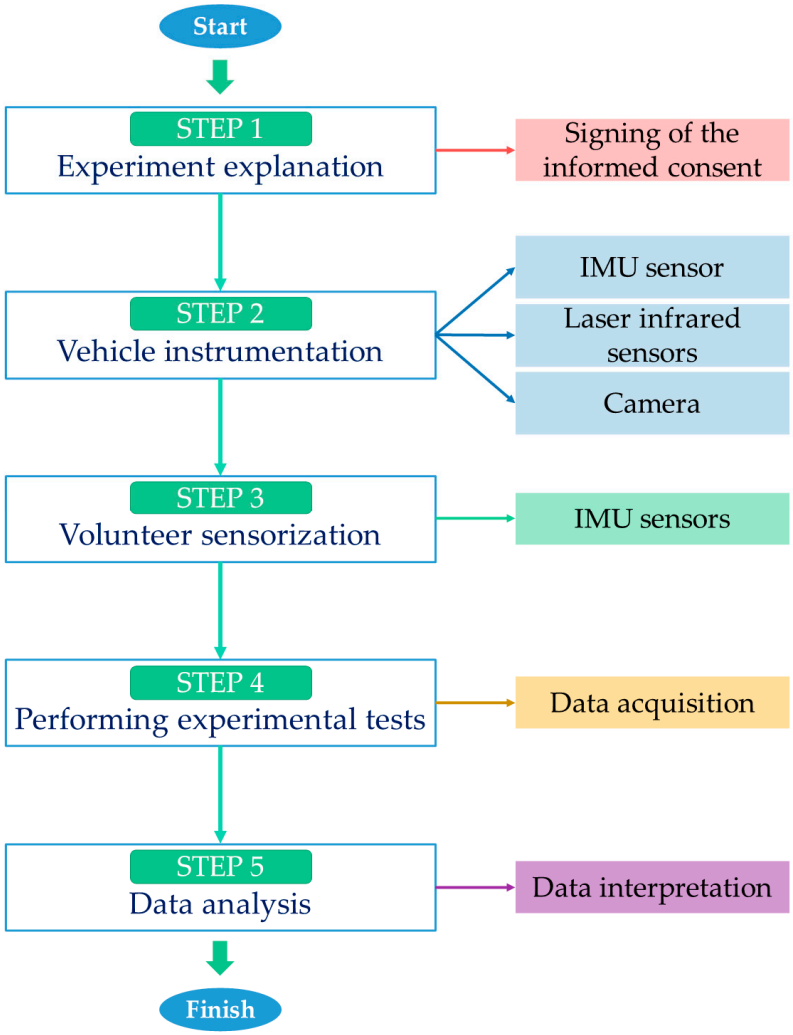

Figure 5. Plan of tests with steps.

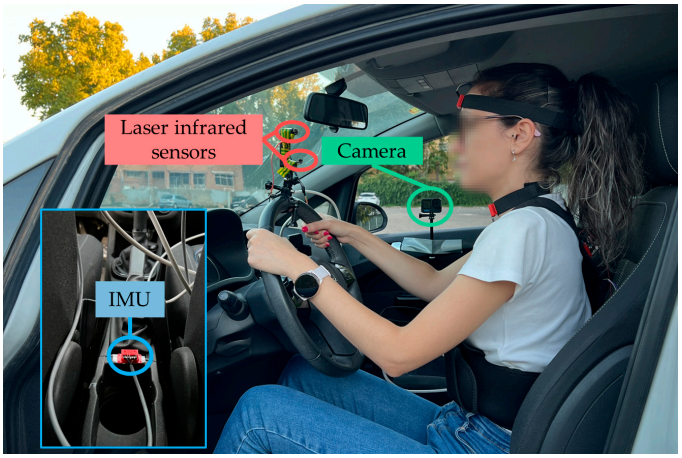

Figure 6. Vehicle instrumentation for a test.

Figure 7. Example of the experimental configuration of wearable units for a test.

Step 4. Performance of the experiments. The measurement instruments were checked and calibrated before the experimental tests. Then, with the vehicle instrumented, the occupant sensorized, and the sensors calibrated, the experiments were conducted. A lower injury level scenario was simulated to avoid injury to the subjects. The volunteers were seated in a normal driving position, with their backs well supported by the seatback, looking straight ahead with their hands placed on the steering wheel and with the three-point seatbelt fastened. In all tests, the seat back angle was set at 24° with respect to the vertical plane and the head restraint was adapted to the height of each volunteer to standardize the procedure. Due to the inclination of the seat with respect to the vertical plane, the distance between the back of the occupant's head and the front surface of the head restraint was 90 mm. The braking test consisted of accelerating the vehicle to a preset constant speed and then performing emergency braking. This type of braking is characterized by the fact that it is fast and abrupt. It is achieved by pressing the brake pedal firmly up to the end of its travel.

In the literature, research results from low-speed pre-impact tests that were conducted with volunteers indicated that the volunteers were exposed to sled accelerations of between 4 and 16.8 m/s^2 [23,39–41]. Consequently, for the experiments, it was decided to assume the lowest possible risk for the participants in the experiments, so braking was performed at 10, 20, and 30 km/h in order to obtain safe values of maximum vehicle acceleration. It should be noted that the threshold of acceleration that can be harmful depends on the subject. Gender, age, physical condition, and previous neck injuries, among other factors, may affect the behavior of the volunteer during braking as well [42].

The volunteers were instructed to be relaxed before braking to prevent their muscles from contracting. This is important because if the volunteer contracts the cervical muscles, the movement of the spine is reduced.

The vehicle used for the experimental tests was an Opel Corsa, which weighs 1124 kg. In addition to the driver, a second person in the co-driver's seat was responsible for controlling the data acquisition system in all tests and supervising the correct execution of the experiment.

Step 5. Analysis of the acquired data. Once the experiments were completed and the data from the sensors were stored, the signals were processed to obtain the parameters necessary to calculate the $NHIC_2$ index.

The tests provide an approximation of the head and neck displacement, as the laser does not always hit the same part of the occupant's head and neck, as reported in the model in Figure 8. As can be seen, the reference points of the sensors change during the experiment due to the bending movement of the head. In Figure 8a, P_h and P_n correspond to the reference points of the head and neck, respectively, before starting the experiment, from which the sensor measures the distance. During the experiment, these points change due to the movement of the head and neck. In the first step of the experiment in Figure 8b, the head moves forward

and the sensor measures the distance to P'_h and P'_n. Then, the head moves backward and in this case, the values of the distance to P''_h and P''_n are obtained, as in Figure 8c.

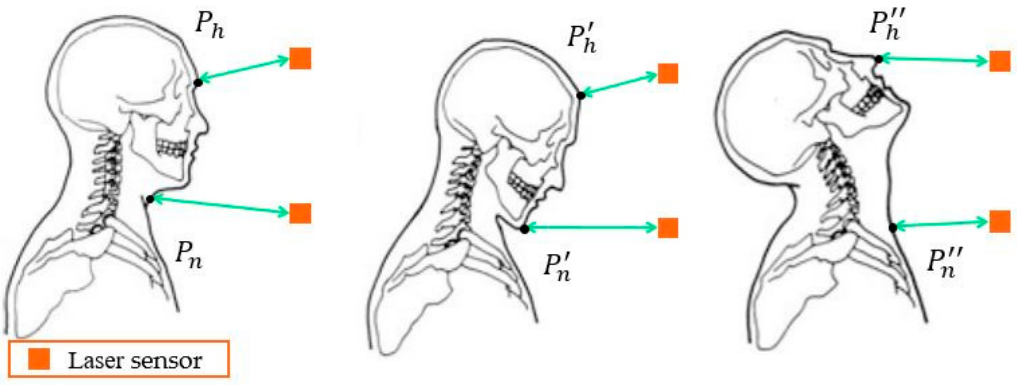

Figure 8. A scheme of the data evaluation of head/neck displacements using laser infrared sensors: (**a**) Neutral posture; (**b**) Forward; (**c**) Backward.

Figure 9 shows snapshots of the relative motion between the head and torso of a volunteer during an experiment.

Figure 9. Snapshot of an experimental test.

Figure 10 shows the map of the scenario of the experiments with indications of the trajectory of the vehicle during tests.

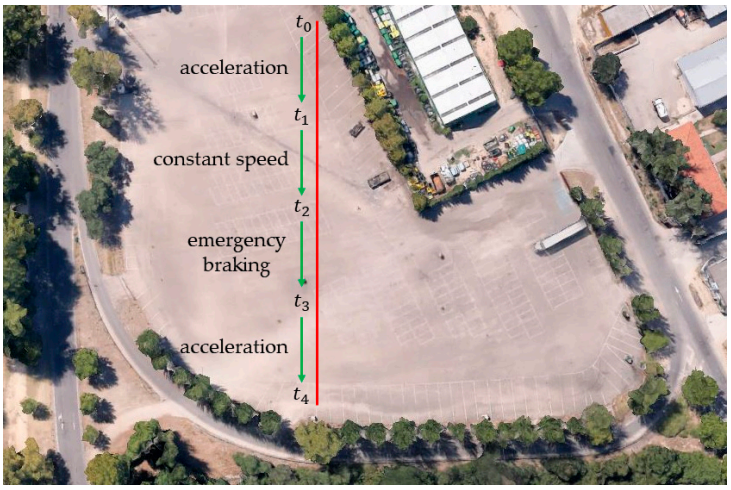

Figure 10. Map of the testing area and vehicle trajectory. t_0 is the start time of the test ($V_v = 0$ m/s); t_1 is the time in which the test speed is reached ($V_v = 2.78,\ 5.56$ or 8.33 m/s); t_2 is the braking time ($V_v = 2.78,\ 5.56$ or 8.33 m/s); t_3 is the final braking time ($V_v = 0$ m/s); t_4 is the end of test time ($V_v = 0$ m/s).

3. Results

Several tests were carried out with volunteers, and representative results are discussed to show the feasibility of the testing procedure. The results of the readings of all sensors during the experiments with a volunteer are shown in plots in Figures 11–13 and Tables 3 and 4. The volunteer was a 32-year-old male, 1.76 m tall, and weighed 77 kg.

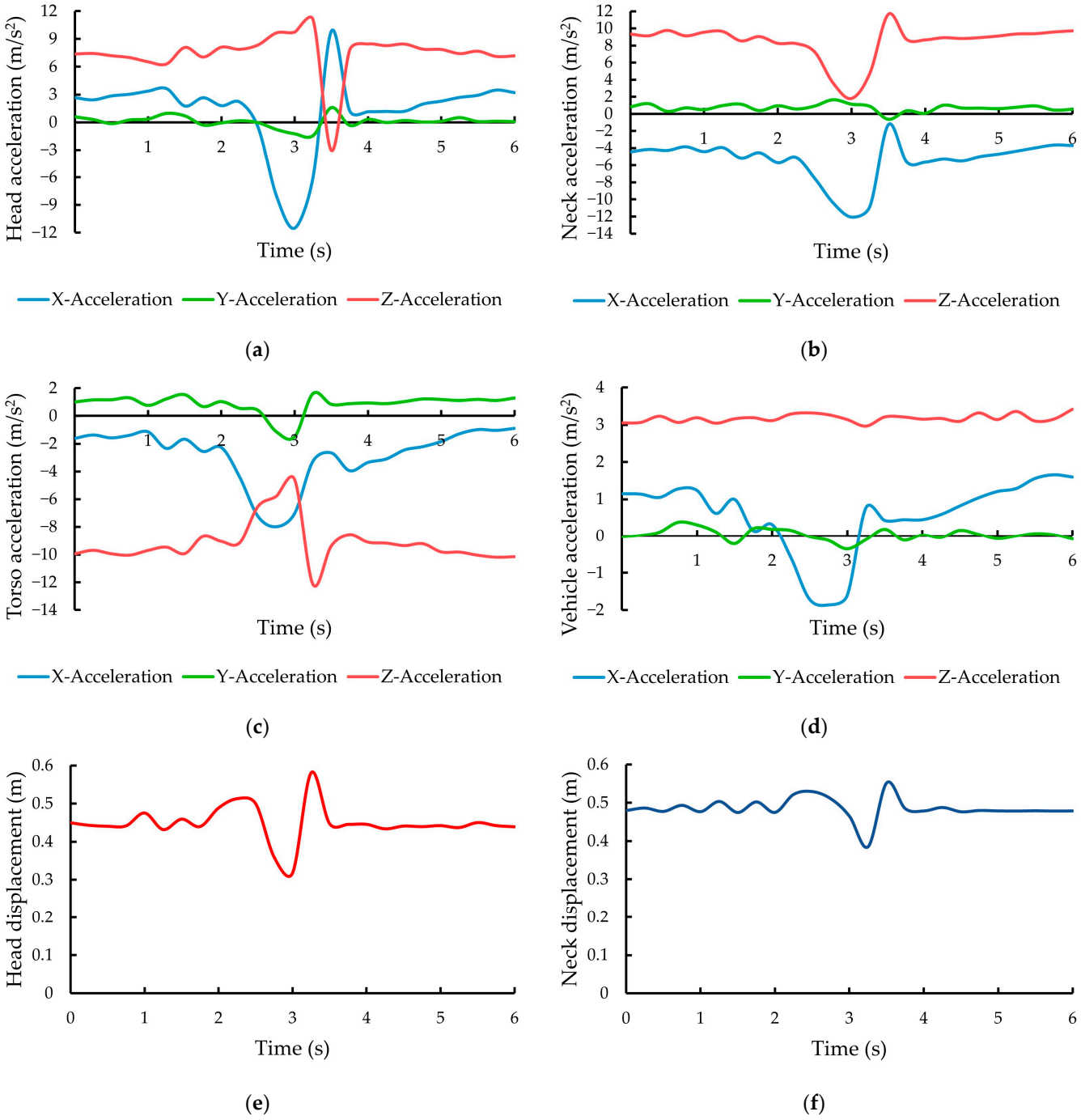

Figure 11. Results acquired during a test at 10 km/h in terms of: (**a**) Head acceleration; (**b**) Neck acceleration; (**c**) Torso acceleration; (**d**) Vehicle acceleration; (**e**) Head displacement; (**f**) Neck displacement.

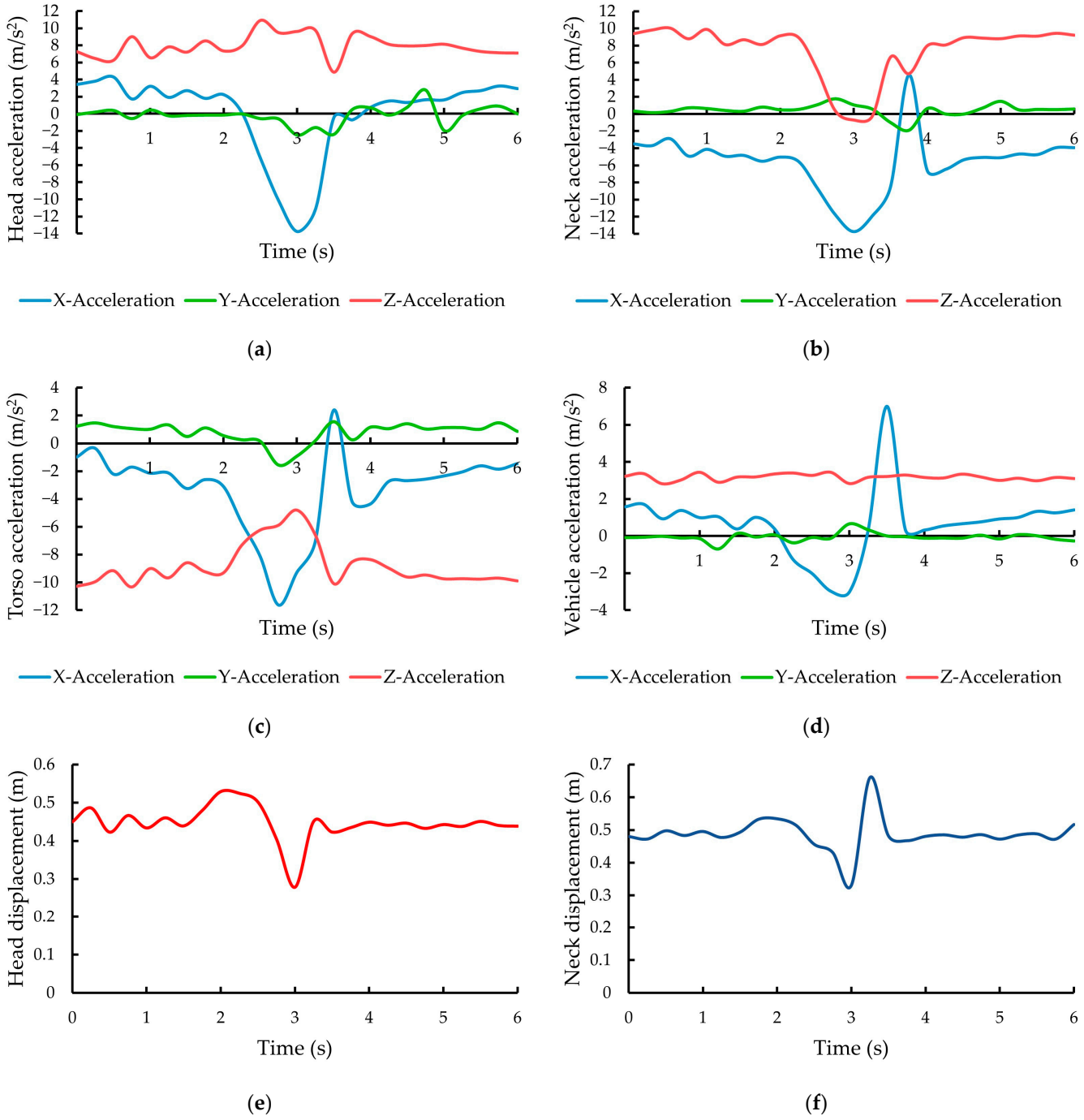

Figure 12. Results acquired during a test at 20 km/h in terms of: (**a**) Head acceleration; (**b**) Neck acceleration; (**c**) Torso acceleration; (**d**) Vehicle acceleration; (**e**) Head displacement; (**f**) Neck displacement.

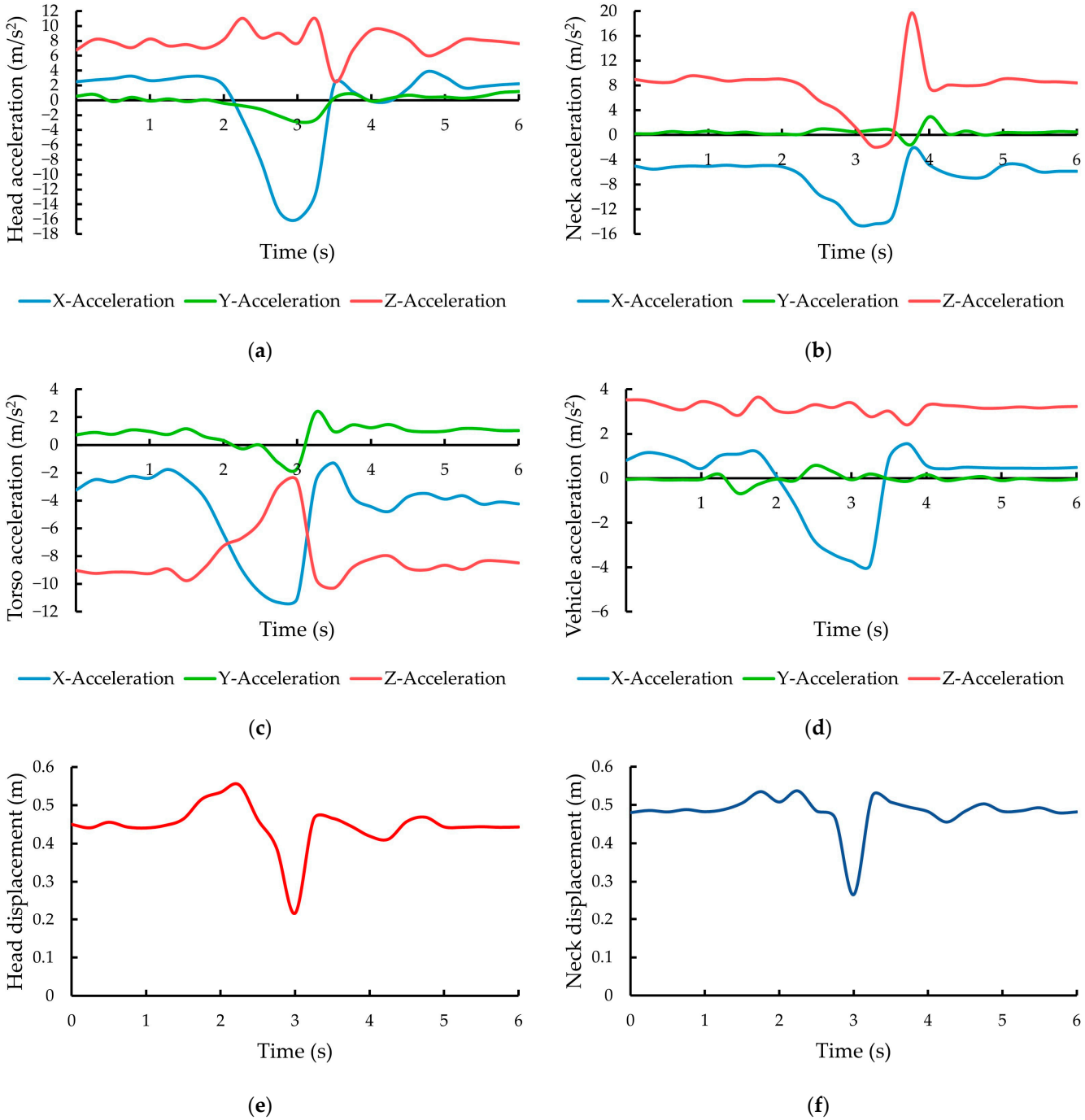

Figure 13. Results acquired during a test at 30 km/h in terms of: (**a**) Head acceleration; (**b**) Neck acceleration; (**c**) Torso acceleration; (**d**) Vehicle acceleration; (**e**) Head displacement; (**f**) Neck displacement.

Table 3. Summary of the data acquired by the IMU and laser sensors during the three example tests at different speeds performed by the same volunteer in Figures 11–13.

Volunteer 1	V_v (m/s)	a_h (m/s^2)	a_t (m/s^2)	a_n (m/s^2)	a_v (m/s^2)	X_{hi} (m)	X_{hf} (m)	X_{ni} (m)	X_{nf} (m)
Test 1	2.78	13.70	5.72	6.96	2.18	0.50	0.32	0.53	0.39
Test 2	5.56	15.99	9.01	8.19	4.03	0.53	0.28	0.53	0.33
Test 3	8.33	19.17	9.57	9.28	5.09	0.55	0.22	0.54	0.27

Table 4. Numerical value of the $NHIC_2$ index for tests evaluated in Table 3.

Test	$NHIC_2$
1	2937
2	1873
3	1491

Figure 11 shows the signals obtained by the different sensors during an experiment at a speed of 10 km/h. The signals correspond to the acceleration of the head, torso, neck, and vehicle taken from the IMU sensors, as well as the distance between the infrared laser sensors and the head and neck of the vehicle occupant. In Figure 11, during the time between 0 and 2 s, the occupant performs normal driving on a straight trajectory on flat ground until the speed at which the experiment is to be performed is reached. Once the test speed is constant, the occupant initiates the emergency braking process. The braking occurs between 2 and 3.75 s. The head moves forward between 2 and 3 s and moves backward between 3 and 3.75 s. Once the braking maneuver is completed, the volunteer returns to the normal driving position and continues driving following a straight trajectory until the end time of the test (6 s).

Referring to Figure 11, during braking in the forward motion of the occupant, the head experiences the maximum acceleration increase in the *X*-axis at 13.70 m/s^2, followed by the neck at 6.96 m/s^2, then the torso at 5.72 m/s^2, and finally the vehicle at 2.18 m/s^2. The displacement of the head is 0.18 m and that of the neck is 0.14 m.

Figure 12 shows the results concerning an experiment at a test speed of 20 km/h. The maximum increase in acceleration in the *X*-axis is again experienced by the head at 15.99 m/s^2, followed by the torso at 9.01 m/s^2, then the neck at 8.19 m/s^2, and finally the vehicle at 4.03 m/s^2. The displacement of the head is 0.25 m and that of the neck is 0.20 m. Braking takes place between 1.75 and 4 s. Forward movement occurs between 1.75 and 3 s and backward movement occurs between 3 and 4 s. This results in a larger braking time than in the previous test.

Figure 13 shows the values obtained during a test run at a speed of 30 km/h. The maximum increase in acceleration in the *X*-axis is experienced by the head at 19.17 m/s^2, followed by the torso at 9.57 m/s^2, then the neck at 9.28 m/s^2, and finally the vehicle at 5.09 m/s^2. The displacement of the head is 0.34 m and that of the neck is 0.27 m. Braking occurs between 1.5 and 4 s. The forward movement is between 1.5 and 3 s and the backward movement is between 3 and 4 s. This is the largest braking maneuver.

Figures 11e, 12e, and 13e show the data that are obtained directly from the infrared laser distance sensor located on the vehicle steering wheel in front of the occupant's head during braking tests at different speeds. Before the test, the average distance between the distance sensor and the vehicle occupant's head is 0.45 m. During braking, the occupant moves forward towards the sensor, exactly 0.32 m (10 km/h), 0.28 m (20 km/h), and 0.22 m (30 km/h) from the sensor. After the test, the occupant continues driving in the normal position. The head displacement was obtained by subtracting the distance between the sensor and the head at the instant before braking and the reading from the minimum distance obtained in the experiment.

Figures 11f, 12f, and 13f show the measurement data acquired with the infrared laser distance sensor placed on the steering wheel of the vehicle in front of the occupant's neck. Before and after the experiment, the average distance between the sensor and the occupant's neck is 0.48 m. The minimum distance obtained between the occupant and the sensor is 0.39 m (10 km/h), 0.33 m (20 km/h), and 0.27 m (30 km/h) during braking. The neck displacement was obtained by subtracting the distance between the sensor and the neck at the instant before braking and the reading of the minimum distance obtained in the experiment.

The recorded situations refer to the model in Figure 6. Table 3 shows a summary of the *X*-axis acceleration increment values of the head (a_h), torso (a_t), neck (a_n), and vehicle (a_v)

during emergency braking, as well as the position of the head (X_{hi} and X_{hf}) and neck (X_{ni} and X_{nf}) before and after the test, corresponding to three different experiments performed by the same volunteer for a vehicle speed at the time of the test (V_v) of 2.78, 5.56, and 8.33 m/s (10, 20, and 30 km/h).

It can be noted from the results in Table 3 that the tendency is to have a larger acceleration of the head, torso, neck, and vehicle as the predetermined speed for emergency braking increases. There is also a trend towards a larger displacement of the head and neck as the test speed increases.

In the 10 km/h test, the acceleration experienced by the head is 139.51% larger than that experienced by the torso and 96.84% larger than that experienced by the neck. In the 20 km/h test, the acceleration of the head is 77.47% larger than that of the torso and 95.24% larger than that of the neck. In the 30 km/h test, the acceleration of the head is 100.31% larger than that of the torso and 106.57% larger than that of the neck.

The data in Table 3 are substituted into Equation (6) to obtain the numerical value of the proposed new criterion, $NHIC_2$, for each test. The resulting values are listed in Table 4. The weight of the co-driver is 48 kg. Therefore, the vehicle weight (m_v) is 1172 kg.

From the results obtained in Table 4, it can be noted that the $NHIC_2$ index decreases as the acceleration experienced during the test increases. This means a lower $NHIC_2$ value is calculated for more severe injuries suffered by the vehicle occupant. In addition, $NHIC_2$ can give a more evident numerical evaluation of the risk as function of more parameters in a risky car accident.

4. Discussion

This paper presents an experimental test that is designed to assess the potential risk of whiplash injury to a vehicle occupant in an emergency braking scenario with reference to a new injury criterion. The design of the experiment is divided into several phases: explanation of the experiment, vehicle instrumentation, occupant sensorization, emergency braking, and, finally, data analysis.

To carry out the experiments, IMU sensors, infrared laser sensors, and a camera were used to obtain head, neck, torso, and vehicle acceleration, head and neck displacement, and occupant movement. These sensors enabled the risks of head and neck injury to be properly analyzed and the new injury criterion to be formulated. The proposed $NHIC_2$ criterion takes into account the consequences for the occupants in terms of head, neck, and torso kinematics and vehicle impact dynamics. The $NHIC_2$ assessment allows for a well-differentiated numerical determination according to additional parameters that have been considered to be the most important determinants of whiplash risk. The proposed new criterion can be used to analyze the risks and consequences of a road traffic crash.

From the experimental results, it can be noted that the head experiences the largest accelerations, followed by the neck and torso, and finally the vehicle. The acceleration in the head, neck, torso, and vehicle increases as the speed at which the emergency braking is executed increases. In terms of displacement, in all tests, the displacement experienced by the head is larger than that experienced by the neck. In all experiments the displacement of the head and neck increases as the speed at which the test is performed increases.

The procedure described in this work can be used to perform reliable biomechanical tests, under real conditions, using low-cost devices. The main limitation of this paper is that a volunteer cannot be exposed to acceleration levels that could cause injury.

A more statistically significant test campaign (with 10–20 volunteers) can be planned in future work for a better investigation of the risk evaluation using the reported test layout.

5. Patents

Ceccarelli, M.; Cafolla, D.; Russo, M.; Garrosa, M.; Díaz, V. No. 102022000022092, Vehicle driver monitoring device, Italy Patent Request, 26 October 2022, No. 202231105, Spain Patent Request, 23 December 2022.

Author Contributions: Conceptualization, M.G., M.C. and V.D.; methodology, M.G. and M.C.; software, M.G.; validation, M.G., M.C. and M.R.; formal analysis, M.G., M.C. and M.R.; investigation, M.G. and M.C.; resources, M.G. and V.D.; data curation, M.G., M.C. and M.R.; writing—original draft preparation, M.G. and M.C.; writing—review and editing, M.G., M.C. and M.R.; visualization, M.G., M.C. and M.R.; supervision, M.G., M.C. and V.D.; project administration, M.G. and M.C.; funding acquisition, M.G., M.C. and V.D. All authors have read and agreed to the published version of the manuscript.

Funding: This research received no external funding.

Data Availability Statement: The data presented in this study are available on request from the corresponding author. The data are not publicly available due to privacy restrictions.

Conflicts of Interest: The authors declare no conflict of interest.

References

1. Freeman, M.D.; Leith, W.M. Estimating the number of traffic crash-related cervical spine injuries in the United States; An analysis and comparison of national crash and hospital data. *Accid. Anal. Prev.* **2020**, *142*, 105571. [CrossRef]
2. Li, F.; Liu, N.S.; Li, H.G.; Zhang, B.; Tian, S.W.; Tan, M.G.; Sandoz, B. A review of neck injury and protection in vehicle accidents. *Transp. Saf. Environ.* **2019**, *1*, 89–105. [CrossRef]
3. Teasell, R.; Mehta, S.; Loh, E. Whiplash Injuries. *Curr. Treat. Options Rheumatol.* **2020**, *6*, 394–405. [CrossRef]
4. Briggs, A.M.; Woolf, A.D.; Dreinhöfer, K.; Homb, N.; Hoy, D.G.; Kopansky-Giles, D.; Åkesson, K.; March, L. Reducing the global burden of musculoskeletal conditions. *Bull. World Health Organ.* **2018**, *96*, 366. [CrossRef] [PubMed]
5. Boström, O.; Svensson, M.Y.; Aldman, B.; Hansson, H.A.; Håland, Y.; Lövsund, P.; Örtengren, T. A new neck injury criterion candidate-based on injury findings in the cervical spinal ganglia after experimental neck extension trauma. In Proceedings of the International Ircobi Conference on the Biomechanics of Impact, Dublin, Ireland, 11–13 September 1996.
6. Ono, K.; Kaneoka, K.; Wittek, A.; Kajzer, J. Cervical injury mechanism based on the analysis of human cervical vertebral motion and head-neck-torso kinematics during low speed rear impacts. *SAE Trans.* **1997**, *106*, 3859–3876. [CrossRef]
7. Meyer, F.; Humm, J.; Purushothaman, Y.; Willinger, R.; Pintar, F.A.; Yoganandan, N. Forces and moments in cervical spinal column segments in frontal impacts using finite element modeling and human cadaver tests. *J. Mech. Behav. Biomed. Mater.* **2019**, *90*, 681–688. [CrossRef] [PubMed]
8. Siegmund, G.P.; Heinrichs, B.E.; Chimich, D.D.; Lawrence, J. Variability in vehicle and dummy responses in rear-end collisions. *Traffic Inj. Prev.* **2005**, *6*, 267–277. [CrossRef] [PubMed]
9. Rueda-Arreguín, J.L.; Ceccarelli, M.; Torres-SanMiguel, C.R. Design of an Articulated Neck to Assess Impact Head-Neck Injuries. *Life* **2022**, *12*, 313. [CrossRef] [PubMed]
10. Yan, Y.; Huang, J.; Li, F.; Hu, L. Investigation of the effect of neck muscle active force on whiplash injury of the cervical spine. *Appl. Bionics Biomech.* **2018**, *2018*, 4542750. [CrossRef]
11. John, J.; Putra, I.P.A.; Iraeus, J. Finite Element Human Body Models to study Sex-differences in Whiplash Injury: Validation of VIVA+ passive response in rear-impact. In Proceedings of the International Ircobi Conference on the Biomechanics of Impact, Porto, Portugal, 14–16 September 2022.
12. Wang, Y.; Jiang, H.; Teo, E.C.; Gu, Y. Finite Element Analysis of Head–Neck Kinematics in Rear-End Impact Conditions with Headrest. *Bioengineering* **2023**, *10*, 1059. [CrossRef]
13. Schmitt, K.U.; Muser, M.H.; Walz, F.H.; Niederer, P.F. N km—A proposal for a neck protection criterion for low-speed rear-end impacts. *Traffic Inj. Prev.* **2002**, *3*, 117–126. [CrossRef]
14. Kleinberger, M.; Sun, E.; Eppinger, R.; Kuppa, S.; Saul, R. Development of improved injury criteria for the assessment of advanced automotive restraint systems. *NHTSA Docket* **1998**, *4405*, 12–17.
15. Heitplatz, F.; Sferco, R.; Fay, P.; Reim, J.; Kim, A.; Prasad, P. An evaluation of existing and proposed injury criteria with various dummies to determine their ability to predict the levels of soft tissue neck injury seen in real world accidents. In Proceedings of the 18th International Technical Conference on the Enhanced Safety of Vehicles, Nagoya, Japan, 19–22 May 2003.
16. Panjabi, M.M.; Wang, J.L.; Delson, N. Neck injury criterion based on intervertebral motions and its evaluation using an instrumented neck dummy. In Proceedings of the International Research Council on the Biomechanics of Injury Conference, Sitges, Spain, 23–24 September 1999.
17. Viano, D.C.; Davidsson, J. Neck displacements of volunteers, BioRID P3 and Hybrid III in rear impacts: Implications to whiplash assessment by a neck displacement criterion (NDC). *Traffic Inj. Prev.* **2002**, *3*, 105–116. [CrossRef]
18. Munoz, D.; Mansilla, A.; Lopez-Valdes, F.; Martin, R. A study of current neck injury criteria used for whiplash analysis proposal of a new criterion involving upper and lower neck load cells. In Proceedings of the 19th Experimental Safety Vehicles Conference, Washington, DC, USA, 6–9 June 2005.
19. Kuppa, S.; Saunders, J.; Stammen, J.; Mallory, A. Kinematically based whiplash injury criterion. *Injury* **2005**, *1*, 1–8.

20. Garrosa, M.; Ceccarelli, M.; Russo, M.; Cafolla, D. Lab Experiences for a Driver Monitoring System. In *New Trends in Medical and Service Robotics. MESROB 2023. Mechanisms and Machine Science*; Tarnita, D., Dumitru, N., Pisla, D., Carbone, G., Geonea, I., Eds.; Springer Nature: Cham, Switzerland, 2023; pp. 109–116. [CrossRef]
21. Ono, K.; Kanno, M. Influences of the physical parameters on the risk to neck injuries in low impact speed rear-end collisions. *Accid. Anal. Prev.* **1996**, *28*, 493–499. [CrossRef] [PubMed]
22. Santos-Cuadros, S.; Fuentes del Toro, S.; Olmeda, E.; San Román, J.L. Surface electromyography study using a low-cost system: Are there neck muscles differences when the passenger is warned during an emergency braking inside an autonomous vehicle? *Sensors* **2021**, *21*, 5378. [CrossRef] [PubMed]
23. Kumar, S.; Ferrari, R.; Narayan, Y.; Jones, T. The effect of seat belt use on the cervical electromyogram response to whiplash-type impacts. *J. Manip. Physiol. Ther.* **2006**, *29*, 115–125. [CrossRef] [PubMed]
24. Panjabi, M.M.; Pearson, A.M.; Ito, S.; Ivancic, P.C.; Wang, J.L. Cervical spine curvature during simulated whiplash. *Clin. Biomech.* **2004**, *19*, 1–9. [CrossRef]
25. Cholewicki, J.; Panjabi, M.M.; Nibu, K.; Babat, L.B.; Grauer, J.N.; Dvorak, J. Head kinematics during in vitro whiplash simulation. *Accid. Anal. Prev.* **1998**, *30*, 469–479. [CrossRef]
26. Grauer, J.N.; Panjabi, M.M.; Cholewicki, J.; Nibu, K.; Dvorak, J. Whiplash produces an S-shaped curvature of the neck with hyperextension at lower levels. *Spine* **1997**, *22*, 2489–2494. [CrossRef]
27. Ono, K.; Kaneoka, K. Motion analysis of human cervical vertebrae during low-speed rear impacts by the simulated sled. *Traffic Inj. Prev.* **1999**, *1*, 87–99. [CrossRef]
28. Eichberger, A.; Steffan, H.; Geigl, B.; Svensson, M.; Boström, O.; Leinzinger, P.E.; Darok, M. Evaluation of the applicability of the neck injury criterion (NIC) in rear end impacts on the basis of human subject tests. In Proceedings of the International Ircobi Conference on the Biomechanics of Impact, Gothenburg, Sweden, 16–18 September 1998.
29. Wheeler, J.B.; Smith, T.; Siegmund, G.P.; Brault, J.R.; King, D.J. Validation of the neck injury criterion (NIC) using kinematic and clinical results from human subjects in rear-end collisions. In Proceedings of the International Ircobi Conference on the Biomechanics of Impact, Gothenburg, Sweden, 16–18 September 1998.
30. Yoganandan, N.; Pintar, F.A. *Frontiers in Whiplash Trauma: Clinical and Biomechanical*; IOS Press: Amsterdam, The Netherlands, 2000; Volume 38.
31. Ivancic, P.C.; Xiao, M. Understanding whiplash injury and prevention mechanisms using a human model of the neck. *Accid. Anal. Prev.* **2011**, *43*, 1392–1399. [CrossRef] [PubMed]
32. Garrosa, M.; Ceccarelli, M.; Díaz, V. Problems and Requirements in Impact Analysis from Vehicle Accidents. In *Advances in Italian Mechanism Science: Proceedings of the 4th International Conference of IFToMM ITALY*; Niola, V., Gasparetto, A., Quaglia, G., Carbone, G., Eds.; Mechanisms and Machine Science; Springer Nature: Cham, Switzerland, 2022; Volume 122, pp. 346–354. [CrossRef]
33. Ceccarelli, M.; Cafolla, D.; Russo, M.; Garrosa, M.; Díaz, V. Vehicle Driver Monitoring Device. Italy Patent Request No. 102022000022092, 26 October 2022.
34. Ceccarelli, M.; Cafolla, D.; Russo, M.; Garrosa, M.; Díaz, V. Dispositivo para la monitorización del conductor de un vehículo. Spain Patent Request No. 202231105, 23 December 2022.
35. Datasheet [Online]. Available online: https://www.alldatasheet.com (accessed on 15 May 2023).
36. Arduino Mega 2560. Available online: https://docs.arduino.cc/hardware/mega-2560 (accessed on 30 June 2023).
37. Garrosa, M.; Ceccarelli, M.; Díaz, V. Propuesta de un nuevo criterio para cuantificar las lesiones en impactos de vehículos. In Proceedings of the Libro de Actas del XV Congreso Iberoamericano de Ingeniera Mecánica, Madrid, Spain, 22–24 November 2022; Volume 3, pp. 291–300. (In Spanish) [CrossRef]
38. Garrosa, M.; Ceccarelli, M.; Díaz, V. Biomechanics in vehicle accidents for risk analysis. *Int. J. Mech. Control* **2023**, *24*, 43–52.
39. Kumar, S.; Narayan, Y.; Amell, T. Analysis of low velocity frontal impacts. *Clin. Biomech.* **2003**, *18*, 694–703. [CrossRef] [PubMed]
40. Kumar, S.; Ferrari, R.; Narayan, Y. Kinematic and electromyographic response to whiplash-type impacts. Effects of head rotation and trunk flexion: Summary of research. *Clin. Biomech.* **2005**, *20*, 553–568. [CrossRef]
41. Hernández, I.A.; Fyfe, K.R.; Heo, G.; Major, P.W. Kinematics of head movement in simulated low velocity rear-end impacts. *Clin. Biomech.* **2005**, *20*, 1011–1018. [CrossRef]
42. Fuentes del Toro, S.; Santos-Cuadros, S.; Olmeda, E.; San Román, J.L. Study of the Emergency Braking Test with an Autonomous Bus and the sEMG Neck Response by Means of a Low-Cost System. *Micromachines* **2020**, *11*, 931. [CrossRef]